Fabrication of Wood Fiber-rubber Composites with Reclaimed Rubber

Dongwei Shao,[a,b] Min Xu,[a,*] Liping Cai,[c] and Sheldon Q. Shi [c]

This research investigated the use of reclaimed rubber (RR) from waste tires to partially replace the rubber compound (RC) when making wood fiber-rubber composites (WRCs). Ninety panels of WRC containing RR were manufactured with RR contents of 0% to 40%, mixing times of 6 min to 14 min, and vulcanizing temperatures of 150 °C to 170 °C. There were three steps, which were the fiber-rubber mixing, tabletting, and vulcanization molding processes. Four regression equations for the tensile strength, elongation at break, hardness, and rebound resilience as functions of the RR content, mixing time, and vulcanizing temperature were derived, and a nonlinear programming model was developed to obtain the optimum panel properties. It was found that when the RR content was within 20%, the wood fibers were well encapsulated and embedded in the RC/RR blends, and the processability of the WRCs were improved by adding RR. The incorporation of RR into the WRCs increased the average tensile strength and hardness by 33.9% and 2.3%, respectively, while the swelling ratio in toluene and 24-h water absorption were reduced by 13% and 42%, respectively.

Keywords: Wood rubber composites (WRCs); Reclaimed rubber (RR); Panel properties; Nonlinear programming model

Contact information: a: Key Laboratory of Bio-Based Material Science and Technology (Northeast Forestry University), Ministry of Education, 150040, Harbin, China; b: College of Mechanical Engineering, Jiamusi University, 154007, Jiamusi, China; c: Mechanical and Energy Engineering department, University of North Texas, Denton 76201, Texas, USA;
** Corresponding author: dl-xumin@nefu.edu.cn*

INTRODUCTION

In recent years, the recycling and disposal of the enormous quantity of difficult to degrade waste rubber (*e.g.*, waste tires) discarded each year has garnered a lot of attention because of environmental concerns (De *et al*. 2006; Ayrilmis *et al.* 2009a; Terzi *et al.* 2009; Hassan 2015). In the past two decades, the rubber industry has been facing a major challenge to find a viable way to recycle the enormous quantity of waste rubber (Adhikari *et al*. 2000; Hernandez-Olivares *et al.* 2002; Chen and Qian 2003; Rooj *et al*. 2011). Driven by green solutions for industry products and the life cycle of consumers using waste tires, an increasing amount of studies have focused on the development of wood-rubber composites (WRCs) during the past decade (Li *et al*. 2005; Zhao *et al*. 2008; Ayrilmis *et al*. 2009a; Zhao *et al*. 2010; Xu and Li 2012; Xu *et al*. 2014). Previous literature indicated that the water resistance, dimensional stability, sound insulation, and energy absorption of WRCs are better compared with neat wood composites.

Wood-rubber composites couple the advantages of both wood and rubber. Wood has a lower density and a better biodegradability compared with inorganic materials (Zhao *et al*. 2008, 2010). Rubber has a low moisture absorption, high compressive performance,

and good sound insulation properties (Ayrilmis *et al*. 2009a; Yang *et al*. 2016). By taking advantage of both materials, WRCs could have multi-functional properties and excellent potential for extended applications. A number of previous studies have been conducted on the manufacturing of WRCs using wood, adhesives, and waste rubber powder with hot-pressing technology (Xu *et al*. 2014; Ding *et al*. 2015; Xia *et al*. 2015). Waste rubber powder is used as a filler and the adhesive is used as a bonding agent. This method has a high production cost and there are concerns about the toxicity and volatility (Shi and Wang 1997; Shi *et al*. 1999). Limited information is available on using rubber compounds (RCs) as a matrix.

In this study, the WRCs were fabricated using rubber processing technology, which includes fiber-rubber mixing, tabletting, and vulcanization molding processes. Instead of adhesives and waste rubber powder, a RC (*i.e.*, un-vulcanized mixing rubber, mainly containing natural rubber (NR), butadiene rubber (BR), butadiene styrene rubber (SBR), and additives) was used to make the composite. As a common material in the tire rubber industry, tire RCs can be used in tough environments and climate conditions because of their ability to withstand high and low temperatures, and high anti-rotting properties (Zhao *et al*. 2011).

To reduce the composite cost, as well as to accentuate the recycling of waste rubber (such as discarded tires), reclaimed rubber (RR) was used to partially replace the RC as part of the rubber in WRCs. Lamminmäki *et al*. (2006) determined that RR presents much better properties than fillers when used as a part of the rubber.

With a plastic characteristic and viscosity, RR can be re-vulcanized (Adhikari *et al.* 2000). However, the drawbacks of RR, such as poor elongation at break (E_b) and rebound resilience (R_r) compared to the raw rubber, could affect the performance of rubber products (Fang *et al.* 2001; Zhang *et al.* 2009). Therefore, it is desirable to determine the optimal RR content in WRCs.

The objective of this research is to investigate the effect of the incorporation of RR into wood fiber (WF) and an RC matrix on the properties of WRCs. A further goal was to determine the optimal RR content and processing parameters.

EXPERIMENTAL

Materials

The WF used in the experiments had a length to width ratio of 5:45, moisture content of 3% to 5%, and was provided by Wooden Forest Products Co., Ltd. (Harbin, China). The RC was supplied by Xingda Rubber Factory (Harbin, China), and contained 30% NR, 6% SBR, 24% BR, 30% carbon black (N330), 1% sulfur, 2.5% zinc oxide, 2% stearic acid, 3% spindle oil, and 1.5% toluene (S.D.). The RR was made from rubber tires that were from light trucks and passenger cars and processed using a continuous shear flow reaction treatment (Xingda Rubber Factory, Harbin, China).

Sample preparation

The WF was initially oven-dried at 103 °C ± 2 °C for 24 h. After the fibers were cooled to room temperature, they were placed in sealed plastic bags until they were used to manufacture the WRCs containing RR (RR-WRCs). Sheets of RC and RR were cut into small pieces (approximately 5 mm^3) so they could mix evenly.

The RR-WRCs were manufactured using rubber processing technology, which includes mixing in a twin rotor mixer, tabletting in an open mill, and sulfide formation in a plate vulcanizing machine. The RR-WRC panels had the dimensions 260 mm × 260 mm × 2 mm (length × width × thickness) and were fabricated at a target density of 1.0 g/cm^3 with RR contents of 0%, 10%, 20%, 30%, and 40% (referred to as R0, R1, R2, R3, and R4, respectively), a mixing time that ranged from 6 min to 14 min, and a vulcanizing temperature that ranged from 150 °C to 170 °C. Six replicate panels were made for each type of composite, which resulted in a total of ninety panels. The control samples (R0) were fabricated using 70% RC and 30% WF.

The RC and RR were premixed at a mixing temperature of 60 °C for 3 min in a twin rotor mixer (XH-409, Zhuosheng Mechanical Equipment Co., Ltd., Dongguan, China). The main rotor speed was 25 rpm, and the speed ratio was 1.3. Then, the WF was gradually added into the mixer and blended for 3 min, 5 min, 7 min, 9 min, and 11 min.

The tabletting process of the mixture was performed using a laboratory two-roller mill (XH-401A, Zhuosheng Mechanical Equipment Co., Ltd., Dongguan, China) for 3 min. The two-roller mill consists of two parallel rollers with different rotation speeds. The speed ratio between the rollers was 1.2, and the gap was 2 mm. The mixing speed, gap between the two rollers, mill roller speed ratio, and sequence of adding the ingredients were kept constant for all of the sample preparations. The sheets from the two-roller mill were conditioned at a temperature of 23 °C ± 2 °C for 24 h in a closed container before vulcanization. Vulcanization was performed in a plate vulcanizing machine (XH-406B, Zhuosheng Mechanical Equipment Co., Ltd., Dongguan, China) at 150 °C, 155 °C, 160 °C, 165 °C, and 170 °C under a pressure of 15 MPa for an optimum curing time (t_{90}), which was also called the vulcanization molding time.

Methods

Characterizations

Tensile specimens that are shown in Fig. 1 were 2-mm-thick, 116-mm-long, 25-mm-wide, and 6-mm-wide at the narrow portion. According to the ISO 37 (2011) standard, a universal testing machine (Instron 4505, Boston, MA, USA) was used determining the tensile strength (T_s) and E_b. The shore type-A durometer (JZ-LX-A, Jingzhuo Company, Yangzhou, China) was utilized for examining the hardness (H_a) of the composite panels according to the standard ISO 7619 (2010). According to the standard ISO 4662 (2009), the elastic impact tester (JZ-6022, Jingzhuo Company, Yangzhou, China) was used to determine R_r with a pendulum of 0.5 J potential energy.

Fig. 1. Morphology of RR-WRCs specimens of dumbbell-shaped

The fracture surface was sputter-coated with gold powder (BAL-TEC, Balzers, Liechtenstein) and then characterized by scanning electron microscopy (SEM; Quanta 200, FEI Company, Hillsboro, USA). The curing characteristics, including the minimum torque (M_L), maximum torque (M_H), scorch time (t_{s2}), and t_{90}, were measured with a no-rotor rheometer (JZ-6029, Jingzhuo Company, Yangzhou, China) according to the standard GB/T 16584 (1996). The authors used the methods of 72-h toluene swelling (De *et al*. 2013) and 24-h water immersion according to the Chinese standard GB/T 11718 (2009) to measure the swelling and water absorption of composites at room temperature. Cut from the vulcanized specimens and dried overnight in a vacuum desiccator, circular samples with a diameter of 10-mm and square samples with a size of 50 mm × 50 mm × 2 mm were prepared. After taking the weights (m_0), these circular and square samples were placed into in toluene and water in bottles for 72 h and 24 h, respectively. After removing the liquids from the sample surfaces with filter paper, the weights (m_1) of these samples were immediately measured. Using the following formula, the absorptions in both the toluene and water (Wa) liquids were obtained,

$$Wa\ (\%) = (m_1 - m_0) \times 100\% / m_0 \quad (1)$$

where m_0 is the weight of the sample before treatment (g) and m_1 is the weight of the sample after treatment (g).

RESULTS AND DISCUSSION

Effect of the RR Content

The properties of the panels prepared with different RR contents at a target panel density of 1 g/cm^3, mixing time of 8 min, and vulcanizing temperature of 160 °C are presented in Table 1. Figures 2 and 3 show that the relationships of the RR content and the *Ts*, *Eb*, *Ha*, and *Rr* were polynomial.

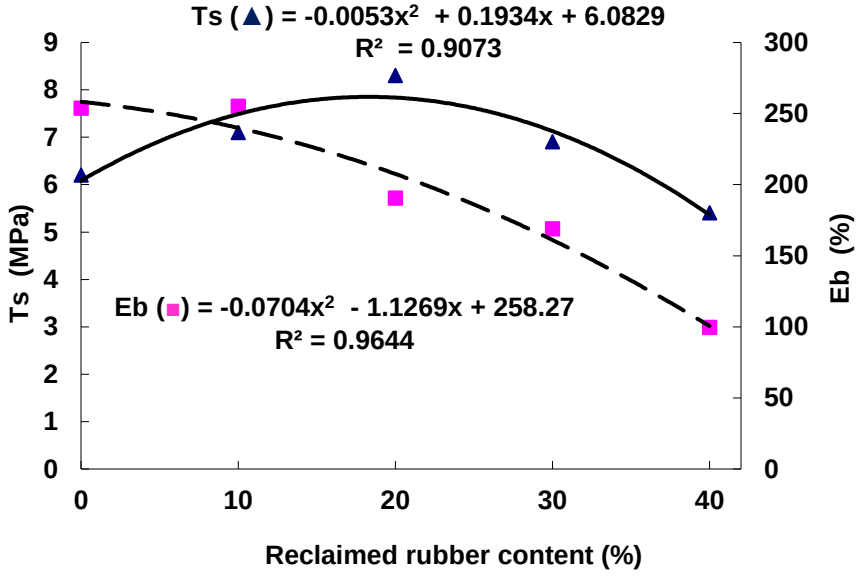

Fig. 2. T_s and E_b as functions of the RR content

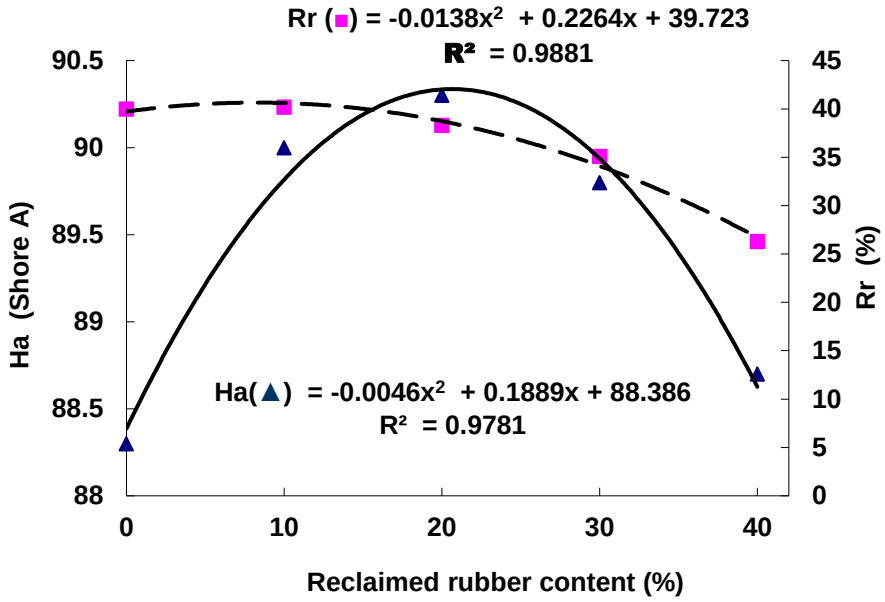

Fig. 3. H_a and R_r as functions of the RR content

The addition of lower amounts of RR (< 20%) improved the mechanical properties of the composites. As the RR content increased from 0% to 20%, T_s and H_a of the composites increased. The increasing trend in T_s was similar to that obtained by De *et al*. (2013). At an RR content of 20%, the maximum T_s and H_a of the composites were obtained, and were 33.9% and 2.3% better compared with the control, respectively. It has been reported that RR has a good plasticity and could be used as a reinforcing agent (De *et al*. 2013). However, if too much RR was added (> 20%), the vulcanization of the rubber and the processing of the composites became difficult because of the lack of curing agents (sulfur) and the increase of inorganic impurity. Some residual cross-linked networks and inorganic impurity in the RR hindered the mobility of the unsaturated segments of the WRCs, which caused the properties of the composites to be reduced.

Table 1. Mechanical Properties of the RR-WRCs with Different RR Contents

RR (%)	T_s (MPa)	E_b (%)	H_a (Shore A)	R_r (%)
0	6.2 (0.3) c[1]	253.6 (8.1) a	88.3 (0.2) e	40.0 (0.1) a
10	7.1 (0.8) b	255.0 (5.5) a	90.0 (0.1) b	40.2 (0.5) a
20	8.3 (0.5) a	190.5 (8.2) b	90.3 (0.1) a	38.3 (0.2) b
30	6.9 (0.5) b	168.8 (7.5) c	89.8 (0.1) c	35.1 (0.5) c
40	5.4 (0.6) d	99.5 (6.8) d	88.7 (0.1) d	26.3 (1.3) d

[1] Groups with the same letters in each column indicate that there was no statistical difference ($p < 0.05$) between the samples according to the Duncan's multiple range test; values in parentheses are the standard deviations

Effect of the Mixing Time

The properties of the panels prepared with different mixing times at a 160 °C vulcanizing temperature, target panel density of 1 g/cm^3, and RR content of 20% are presented in Table 2. The polynomial relationships between the mixing time and the T_s, E_b, H_a, and R_r are illustrated in Figs. 4 and 5.

Table 2. Properties of the RR-WRCs with Different Mixing Times

Mixing Time (min)	T_s (MPa)	E_b (%)	H_a (Shore A)	R_r (%)
6	4.5 (0.3) c[1]	71.5 (7.6) d	65.4 (0.8) d	22.1 (0.5) c
8	7.8 (0.3) a	192.3 (6.4) a	87.1 (0.4) a	38.4 (0.6) a
10	7.6 (0.5) a	189.6 (5.3) a	84.7 (0.4) b	38.6 (0.4) a
12	7.4 (0.2) a	180.4 (6.4) b	82.3 (1.4) c	38.1 (0.1) a
14	5.7 (0.5) b	120.7 (5.6) c	63.8 (1.8) e	30.5 (0.7) b

[1] Groups with the same letters in each column indicate that there was no statistical difference ($p < 0.05$) between the samples according to the Duncan's multiple range test; values in parentheses are the standard deviations

With an increase in the mixing time from 6 min to 14 min, the mechanical properties of the composites increased at first, and then they decreased. The mechanical properties were lowest at a mixing time of 6 min, possibly because the mixing time was too short for sufficient contact between the rubber and WF to occur. The T_s reached a maximum at 8 min, the R_r reached a maximum at 11 min, and the E_b and H_a reached maximum values at 10 min. However, when the mixing time was too long (over 11 min), the mixture temperature increased too fast, and created a radial temperature gradient in the mixing chamber that caused scorching. As a result, the T_s, E_b, H_a, and R_r decreased when the mixing time was longer than 11 min.

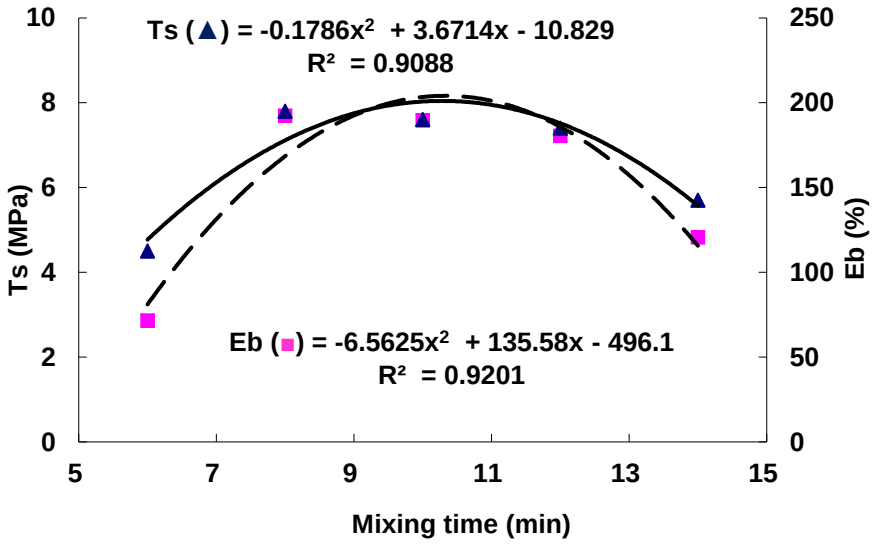

Fig. 4. *Ts* and *Eb* as functions of the mixing time

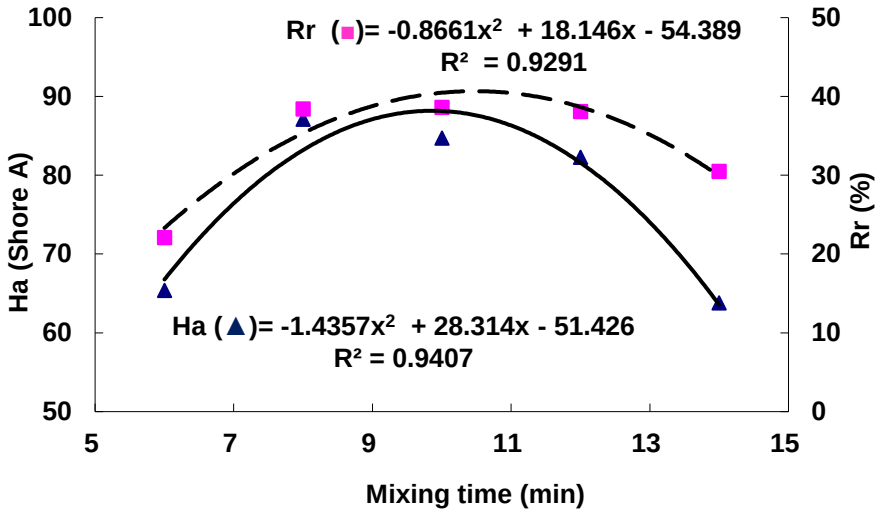

Fig. 5. H_a and R_r as functions of the mixing time

Effect of the Vulcanizing Temperature

The properties of the panels prepared at a target panel density of 1 g/cm^3 with different vulcanizing temperatures, an RR content of 20%, and mixing time of 8 min are presented in Table 3. The polynomial relationships between the vulcanizing temperature and the T_s, E_b, H_a, and R_r are illustrated in Figs. 6 and 7.

The mechanical properties of the composites were relatively low at a vulcanizing temperature of 150 °C, possibly because of poor curing conditions and insufficient contact between the rubber and WF. The mechanical properties increased with the vulcanizing temperature at first. The R_r reached a maximum value at the vulcanizing temperature of approximately 157 °C, the T_s and H_a reached maximum values at 160 °C, and the E_b reached a maximum value at the vulcanizing temperature of 162 °C. However, higher vulcanizing temperatures (over 162 °C) probably dried out the wood cell antrum, which made the WFs fragile (Zhao et al. 2008). As a result, the T_s, E_b, H_a, and R_r decreased when the vulcanizing temperature was above 162 °C.

Table 3. Properties of the RR-WRCs with Different Vulcanizing Temperatures

Vulcanizing Temperature (°C)	T_s (MPa)	E_b (%)	H_a (Shore A)	R_r (%)
150	4.1 (0.3) c[1]	136.5 (14.3) c	74.5 (0.3) e	35.3 (0.6) c
155	6.7 (0.2) b	180.4 (8.2) a	88.3 (0.7) b	39.2 (0.1) a
160	7.9 (0.6) a	189.3 (5.2) a	90.1 (0.2) a	38.8 (0.4) a
165	6.2 (0.5) b	178.2 (13.6) a	84.5 (0.5) c	37.5 (0.7) b
170	3.7 (0.8) c	162.5 (7.8) b	76.3 (0.4) d	19.5 (0.4) d

1 Groups with the same letters in each column indicate that there was no statistical difference ($p < 0.05$) between the samples according to the Duncan's multiple range test; values in parentheses are the standard deviations

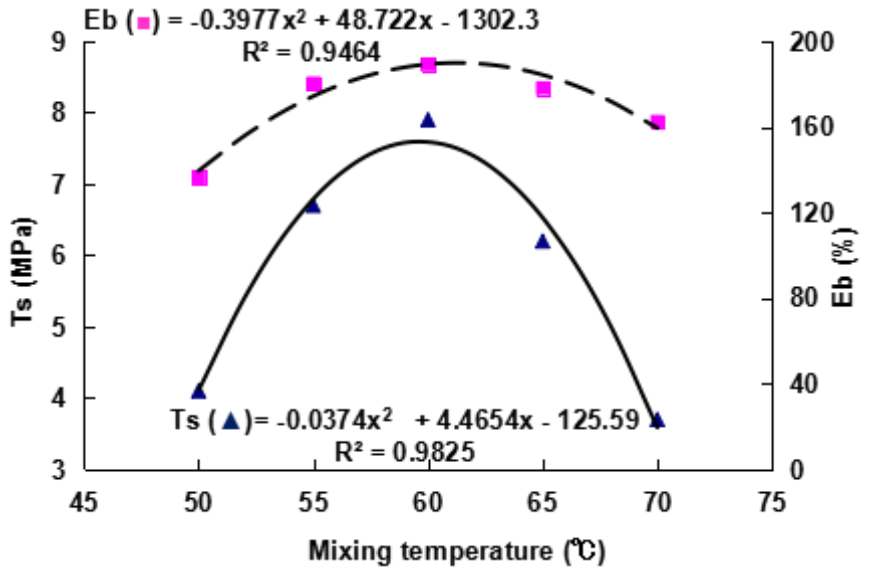

Fig. 6. *Ts* and *Eb* as functions of the vulcanizing temperature

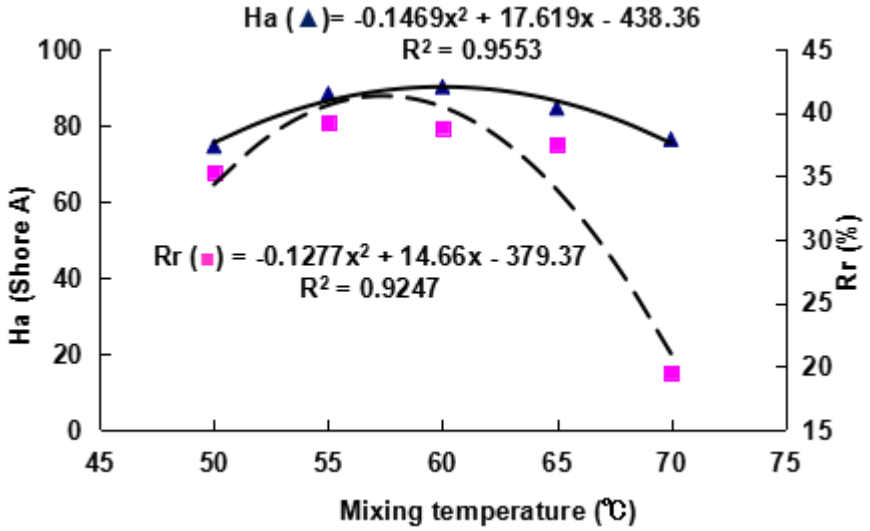

Fig. 7. *Ha* and *Rr* as functions of the vulcanizing temperature

Nonlinear Regression Model

Based on the experimental data, four regression equations for the T_s, E_b, H_a, and R_r (as functions of the RR content, mixing time, and vulcanizing temperature) were obtained and are shown below,

$$T_s = -932.6514 + 0.1511x_1 - 0.0042x_1^2 + 3.9714x_2 - 0.1960x_2^2 + 11.5206x_3 - 0.0361x_3^2 \quad R^2 = 0.9286 \quad (2)$$

$$E_b = -10001 - 3.5948x_1 - 0.00873x_1^2 + 150.5329x_2 - 7.4321x_2^2 + 118.1859x_3 - 0.3662x_3^2 \quad R^2 = 0.9013 \quad (3)$$

$$H_a = -3023.3 - 0.1518x_1 + 0.0039x_1^2 + 31.8171x_2 - 1.6394x_2^2 + 37.0365x_3 - 0.1158x_3^2 \quad R^2 = 0.8929 \quad (4)$$

$$R_r = -2460.1 + 0.1299x_1 - 0.0114x_1^2 + 20.2650x_2 - 0.9892x_2^2 + 30.68x_3 - 0.0980x_3^2 \quad R^2 = 0.8907 \quad (5)$$

where x_1 is the RR content (%), x_2 is the mixing time (min), x_3 is the vulcanizing temperature (°C), and R^2 is the coefficient of determination of each regression equation.

Using these four equations, the T_s, E_b, H_a, and R_r of a panel can be predicted based on the production conditions (RR content, mixing time, and vulcanizing temperature).

Optimization

When mill personnel want to alter the production parameters for a special application, a nonlinear programming model can be used as a guideline to set the production parameters. In the case of flooring for children, the panel material needs the highest T_s, and proper H_a and elasticity to prevent children from being hurt. In cases where a maximum T_s is desired for the panels, the standard for rubber and plastic floor covering materials (Chinese standard HG/T 3747.1 (2011)) requires minimum T_s, E_b, H_a, and R_r values of 0.3 MPa, 40%, 75 Shore A, and 38%, respectively. The nonlinear programming model (Eqs. 6 to 9) was found to be,

$$F(x) = -932.6514 + 0.1511x_1 - 0.0042x_1^2 + 3.9714x_2 - 0.1960x_2^2 + 11.5206x_3 - 0.0361x_3^2 \quad (6)$$

Eq. 6 was subject to:

$$-10001 - 3.5948x_1 - 0.00873x_1^2 + 150.5329x_2 - 7.4321x_2^2 + 118.1859x_3 - 0.3662x_3^2 \geq 40\% \quad (7)$$

$$-3023.3 - 0.1518x_1 + 0.0039x_1^2 + 31.8171x_2 - 1.6394x_2^2 + 37.0365x_3 - 0.1158x_3^2 \geq 75 \quad (8)$$

$$-2460.1 + 0.1299x_1 - 0.0114x_1^2 + 20.2650x_2 - 0.9892x_2^2 + 30.68x_3 - 0.0980x_3^2 \geq 38 \quad (9)$$

and the experimental condition constraints were as follows:

$0 \leq x_1 \leq 40$
$6 \leq x_2 \leq 14$
$150 \leq x_3 \leq 170$

The optimal values for x_1, x_2, and x_3 were 18%, 10 min, and 160 °C, respectively. The results indicated that a maximum T_s of 7.96 MPa for the panel was obtained with a RR content of 18%, vulcanizing temperature of 160 °C, and target panel density of 1 g/cm^3. This resulted in the E_b, H_a, and R_r for the panel being 228.61%, 91.82 Shore A, and 42.27%, respectively, which were greater than the requirements stipulated by the standard HG/T 3747.1 (2011).

Micro-morphology of the RR-WRCs

The SEM photos of the cryogenically fractured surface parallel to the thickness of the RC, R0, R1, R2, R3, and R4 samples are shown in Fig. 8. A homogeneous structure is shown in Fig. 8a for the pure RC sample. Based on Figs. 8b to 8f of the WRCs, the WFs were easily identified and embedded in the RC/RR matrices. In Figs. 8b to 8d, wetted fibers with better interfacial bonding were seen between the WFs and RC/RR matrices, which confirmed there was an optimum reinforcing effect caused by the addition of RR.

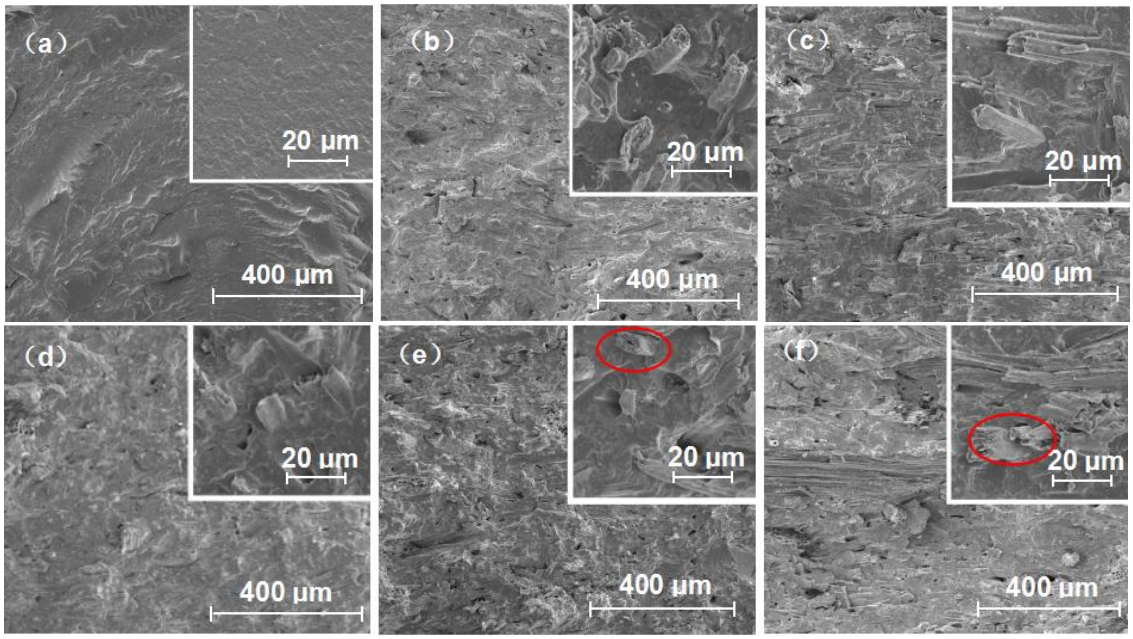

Fig. 8. SEM images of (a) pure RC; (b) control formulation R0 (WRC containing 30% WF and 70% RC); (c) RR-WRC containing 10% RR; (d) RR-WRC containing 20% RR; (e) RR-WRC containing 30% RR; and (f) RR-WRC containing 40% RR

When the RR content was less than 20%, smaller fragments and shorter chains in the RR acted as plasticizers (De *et al.* 2013), which could help with the mixing process between WFs and RC/RR matrices. However, when a greater amount of RR was added (≥ 30%), the distributions of the WF became non-uniform and the fracture surface became rough. From the micrographs shown in Figs. 8e to 8f, cracks were observed between the WF and RC/RR blends (see circled areas in Figs. 8e and 8f). These cracks could have been the reason that poor properties (such as the T_s and E_b) were obtained for the R3 and R4 samples.

Curing Characteristics of the RR-WRCs

The processability of the composites is related to the curing characteristics. The curing curves and characteristic parameters of the RR-WRCs at 160 °C are shown in Fig. 9 and Table 4, respectively.

The M_L, given in Table 4, is related to the material flow characteristics, such as the viscosity. When the M_L value was smaller, then the liquidity of the un-vulcanized rubber mixture was better. The M_H is a measure of the elastic modulus related to the crosslinking density and stiffness of the materials (García *et al.* 2007). Figure 9 shows that when the RR content varied from 0% to 20% and the curing time increased, the torque of the R0, R1, and R2 curves initially decreased, and then increased, before finally levelling off. The initial decrease in the torque could have been because of the softening of the rubber matrix, while the increase in the torque might have been because of the crosslinking of the rubber. The levelling off indicated that the curing was completed. Figure 9 shows that the curing curve for the composites with 20% RR was much closer to that of the R0 control sample compared with the R1 sample. When an excessive amount of RR was added (> 20%), R3 and R4 were un-vulcanized because of the lack of curing agents (sulfur). This result was in agreement with the results of the optimized mechanical properties.

Table 4. Curing Characteristics of the RR-WRCs

RR Content (%)	M_L (N·m)	M_H (N·m)	t_{s2} (min)	t_{c90} (min)	Curing Rate Index (min^{-1})
0	0.89 (0.07)[1]	2.07 (0.16)	1.95 (0.28)	6.12 (0.21)	23.98 (0.17)
10	0.59 (0.03)	1.10 (0.23)	2.88 (0.17)	6.42 (0.42)	28.25 (0.32)
20	0.85 (0.13)	1.39 (0.09)	2.60 (0.11)	5.15 (0.34)	39.20 (0.27)
30	0.52 (0.04)	0.62 (0.17)	0.11 (0.02)	4.66 (0.24)	21.98 (0.04)
40	0.41 (0.15)	0.43 (0.12)	0.00 (0.01)	19.10 (0.31)	5.23 (0.13)

Note: [1] Values in parentheses are the standard deviations

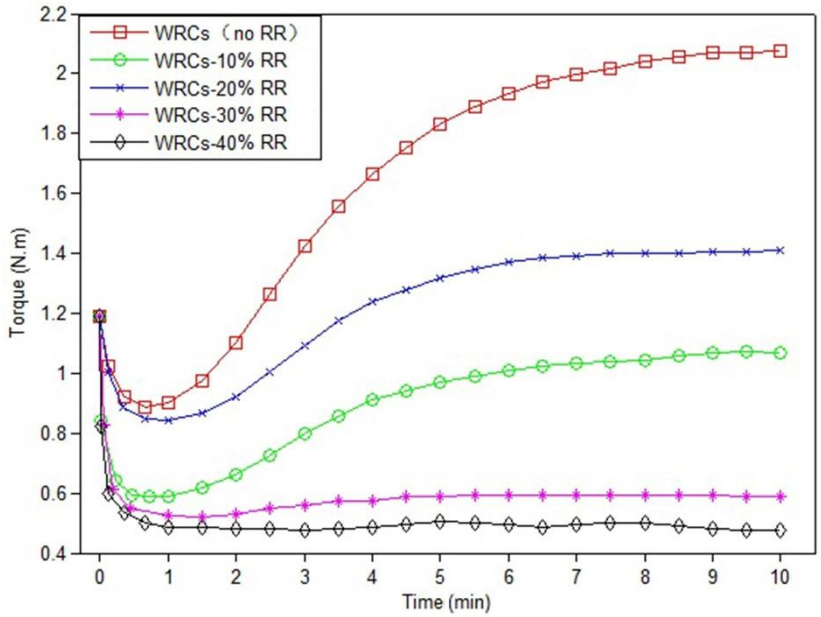

Fig. 9. Cure-curves of the RR-WRCs

Table 4 shows that, compared with the R0 control sample, the M_L and M_H of the RR-WRCs decreased slightly. The lower M_L values indicated the RR-WRCs had a better liquidity and processability in the un-vulcanized rubber mixture. The lower M_H values suggested that the elastic modulus was lower in the composites with higher RR contents. The small fragments and short chains in the RR acted as plasticizers, which decreased the viscosity and torque of the RR-WRCs, and increased their flowability. It was observed in Table 4 that adding more RR reduced the M_H. The 20% RR content resulted in the highest MH value compared with the other RR contents. Further vulcanization occurred for the RR-WRC specimens with a 20% RR content because of the greater amount of curing agents. This result agrees with the results reported by Li *et al.* (2005).

The t_{s2} is the time when the rubber starts to vulcanize. The t_{90} is the vulcanization molding time of the composites. Longer curing times indicated that curing was slower and resulted in lower yields. Table 4 shows that the t_{s2} and t_{90} increased slightly as the RR content increased to 10%, and then decreased when the RR content continued to increase. In particular, when the t_{s2} decreased to 0 min for the composites with 40% RR, the t_{90} increased to 19.10 min. The increased t_{s2} and t_{90} values indicated that the cross-linking reactions were slowed down by adding small amounts of RR (< 10%). The WFs contain hydrophobic groups (-OH), which absorb the curing agents, and thus reduce the active

agent (Ooi *et al*. 2013). When the RR content ranged from 10% to 20%, the lower t_{s2} and t_{90} values in the blends indicated that the cross-linking reactions started earlier with a higher curing rate. The maximum curing rate was obtained when a 20% RR loading was used. A reaction between the RR and WRCs resulted in a product that catalyzed the cross-linking reactions. In addition, diffusion of the accelerator from the RR into the WRCs could have shortened the t_{s2} and t_{90}. However, the decreased t_{s2} and increased t_{90} when 40% RR was used suggested that the vulcanization process was the slowest, no vulcanization occurred, and the curing rate was minimized.

Swelling Ratio

The swelling ratios of the R0, R1, R2, R3, and R4 samples in toluene as a function of the RR content are presented in Table 5.

Table 5. Swelling Ratio of the RR-WRCs

Swelling Ratio (%)	R0	R1	R2	R3	R4
Value	118.9 (4.3)[1]	112.3 (1.8)	103.4 (3.1)	103.7 (0.2)	105.4 (1.2)

Note: [1] Values in parentheses are the standard deviations

When the RR content increased from 0% to 20%, the swelling ratio decreased to the minimum value of 13%. As the RR content continued to increase, the swelling ratio increased, which indicated that 20% was the optimum RR content. There was a decrease in the swelling ratio, in which the RR was assumed as a part of the rubber. When the RR content was higher, there were more active cross-linking sites and lower swelling ratios for the composites. The lower swelling ratios suggested that a higher cross-linking density was obtained (Li *et al.* 2005). This could have been an explanation for the improved mechanical properties and higher MH of the RR-WRCs. When the RR content was higher than 20%, the swelling ratio increased. This was because of the migration of sulfur being obstructed by short molecules and small fragments in the RR.

Water Absorption

The results of the 24-h water absorption of RR-WRCs are displayed in Table 6.

Table 6. Water Absorption of the RR-WRCs

Water Absorption (%)	R0	R1	R2	R3	R4
Value	1.09 (0.12)[1]	0.84 (0.06)	0.63 (0.08)	2.37 (0.22)	2.78 (0.03)

Note: [1] Values in parentheses are the standard deviations

The water absorption of the composites increased slightly compared with the corresponding unfilled sheets. The increased water absorption of the composites was due to the hydrophilic nature of the WFs. The weights of the samples first decreased, reached a minimum value of 42% at the 20% RR content, and then increased as the RR content continued to increase. The lower water absorption suggested that the WFs were well encapsulated in the RC/RR blends. The higher water absorption could have been connected to the degradation of a large amount of RR, which led to the presence of a small amount of the surface being partially encapsulated WF with a hydrophilic nature (Ayrilmis *et al.*

2009b). However, for all of the composite samples, the water absorption ranged from 0.5% to 3%, which was a significant reduction compared with commercial wood-based composites. It was indicated that most of the WFs were encapsulated in the rubber matrix, which has an excellent hydrophobicity.

CONCLUSIONS

1. A reclaimed rubber (RR) content of less than 20% increased the mechanical properties and processability, and reduced the swelling ratio in toluene and 24-h water absorption of the composites. These improvements were caused by the increase in interfacial bonding between the rubber and wood fibers (WFs), as shown in the micro-morphology and curing characteristics analysis for wood fiber composites (WFCs).
2. Four regression equations (Eqs. 2 to 5) were developed. Given the manufacturing conditions (RR content, mixing time, and vulcanizing temperature), the properties of the RR-WRCs can be estimated.
3. With nonlinear programming, the desired tensile strength (T_s), elongation at break (E_b), hardness (H_a), or rebound resilience (R_r) can be obtained under certain practical constraints. The optimal manufacturing conditions of an 18% RR content, 10-min mixing time, and 160 °C vulcanizing temperature resulted in a maximum T_s (7.96 MPa) for the RR-WRC panels.

ACKNOWLEDGMENTS

This research was supported by the National Natural Science Foundation of China (31670574).

REFERENCES CITED

Adhikari, B., De, D., and Maiti, S. (2000). "Reclamation and recycling of waste rubber," *Prog. Polym. Sci.* 25(7), 909-948. DOI: 10.1016/S0079-6700(00)00020-4

Ayrilmis, N., Buyuksari, U., and Avci, E. (2009a). "Utilization of waste tire rubber in the manufacturing of particleboard," *Mater. Manuf. Process.* 24(6), 688-692. DOI: 10.1080/10426910902769376

Ayrilmis, N., Buyuksari, U., and Avci, E. (2009b). "Utilization of waste tire rubber in manufacture of oriented strandboard," *Waste Manage.* 29(9), 2553-2557. DOI: 10.1016/j.wasman.2009.05.017

Chen, F. Z., and Qian, J. L. (2003). "Studies of the thermal degradation of waste rubber," *Waste Manage.* (Oxford) 23, 463-467. DOI: 10.1016/S0956-053X(03)00090-4

De, D., Das, A., De, D., Dey, B., Debnath, S. C., and Roy, B. C. (2006). "Reclaiming of ground rubber tire (GRT) by a novel reclaiming agent," *Eur. Polym. J.* 42(4), 917-927. DOI: 10.1016/j.eurpolymj.2005.10.003

De, D., Panda, P. K., Roy, M., and Bhunia, S. (2013). "Reinforcing effect of reclaim rubber on natural rubber/polybutadiene rubber blends," *Mater. Design* 46, 142-150. DOI: 10.1016/j.matdes.2012.10.014

Ding, Z., Shi, S. Q., Zhang, H., and Cai, L. (2015). "Electromagnetic shielding properties of iron oxide impregnated kenaf bast fiberboard," *Compos. Part B-Eng.* 78, 266-271. DOI: 10.1016/j.compositesb.2015.03.044

Fang, Y., Zhan, M., and Wang, Y. (2001). "The status of recycling of waste rubber," *Mater. and Des.* 22(2), 123-128. DOI:10.1016/S0261-3069(00)00052-2

García, D., López, J., Balart, R., Ruseckaite, R. A., and Stefani, P. M. (2007). "Composites based on sintering rice husk-waste tire rubber mixtures," *Mater. Design* 28(7), 2234-2238. DOI: 10.1016/j.matdes.2006.06.001

Hassan, M. H. (2015). "Synergistic effect of montmorillonite-clay and gamma irradiation on the characterizations of waste polyamide copolymer and reclaimed rubber powder nanocomposites," *Compos. Part B-Eng.* 79, 28-34. DOI: 10.1016/j.compositesb.2015.01.046

Hernandez-Olivares, F., Barluenga, G., Bollati, M., and Witoszek, B. (2002). "Static and dynamic behavior of recycled tire rubber-filled concrete," *Cem. Concr. Res.* 32, 1587-1596. DOI: 10.1016/S0008-8846(02)00833-5

GB/T 11718 (2009). "Medium density fibreboard," Standardization Administration of China, Beijing, China.

GB/T 16584 (1996). "Rubber, measurement of vulcanization characteristics with rotorless curemeters," Standardization Administration of China, Beijing, China.

HG/T 3747.1 (2011). "Rubber and plastic floor covering material. Part 1: Rubber floor coverings," Chemical Industry Standard of China, Beijing, China.

ISO 37 (2011). "Rubber, vulcanized or thermoplastic – Determination of tensile stress-strain properties," International Organization for Standardization, Geneva, Switzerland.

ISO 4662 (2009). "Rubber, vulcanized or thermoplastic – Determination of rebound resilience," International Organization for Standardization, Geneva, Switzerland.

ISO 7619 (2010). "Rubber, vulcanized or thermoplastic – Determination of indentation hardness-Part 1: Durometer method (Shore hardness)," International Organization for Standardization, Geneva, Switzerland.

Lamminmäki, J., Li, S., and Hanhi, K. (2006). "Feasible incorporation of devulcanized rubber waste in virgin natural rubber," *J. Mater. Sci.* 41(24), 8301-8307. DOI: 10.1007/s10853-006-1010-y

Li, S., Lamminmäki, J., and Hanhi, K., (2005). "Improvement of mechanical properties of rubber compounds using waste rubber/virgin rubber," *Polym. Eng. Sci.* 45(9), 1239-1246. DOI: 10.1002/pen.20402

Ooi, Z. X., Ismail, H., and Bakar, A. A. (2013). "Optimisation of oil palm ash as reinforcement in natural rubber vulcanisation: A comparison between silica and carbon black fillers," *Polym. Test.* 32(4), 625-630. DOI: 10.1016/j.polymertesting.2013.02.007

Rooj, S., Basak, G. C., Maji, P. K., and Bhowmick, A. K. (2011). "New route for devulcanization of natural rubber and the properties of devulcanized rubber," *J. Polym. Environ.* 19, 382-390. DOI: 10.1007/s10924-011-0293-5

Shi, S. Q., Gardner, D. J., and Wang, J. Z. (1999). "Effect of the addition of polymer fluff on the mechanical and physical properties of wood fiberboard," *Forest Prod. J.* 49(2),

32-38.
Shi, S. Q., and Wang, J. Z. (1997). "Utilization of polymer automobile fluff in wood fiberboard," *Journal of Solid Waste Technology and Management* 24(4), 188-195.
Terzi, E., Köse, C., Büyüksarı, Ü., Avcı, E., Ayrılmış, N., and Kartal, S. N. (2009). "Evaluation of possible decay and termite resistance of particleboard containing waste tire rubber," *Int. Biodeter. Biodegr.* 63(6), 806-809. DOI: 10.1016/j.ibiod.2009.01.010
Xia, C., Shi, S. Q., and Cai, L. (2015). "Vacuum-assisted resin infusion (VARI) and hot pressing for $CaCO_3$ nanoparticle treated kenaf fiber reinforced composites," *Compos. Part B-Eng.* 78, 138-143. DOI: 10.1016/j.compositesb.2015.03.039
Xu, M., and Li, J. (2012). "Effect of adding rubber powder to poplar particles on composite properties," *Bioresource Technol.* 118, 56-60. DOI: 10.1016/j.biortech.2012.02.041
Xu, M., Li, J., Shi, S. Q., and Cai, L. (2014). "Property enhancement of wood-rubber composites by microwave treatment of rubber particles," *Wood Fiber Sci.* 46(4), 547-554.
Yang, H., Li, F., Chan, T. W., Liu, L., and Zhang, L. (2016). "Effect of nanofiller shape on viscoelasticity of rubber nanocomposite investigated by FEA," *Compos. Part B-Eng.* 92, 160-166. DOI: 10.1016/j.compositesb.2015.12.002
Zhang, X., Lu, C., and Liang, M. (2009). "Properties of natural rubber vulcanizates containing mechanochemically devulcanized ground tire rubber," *J. Polym. Res.* 16(4), 411-419. DOI: 10.1007/s10965-008-9243-x
Zhao, J., Wang, X.-M., Chang, J.-M., Yao, Y., and Cui, Q. (2010). "Sound insulation property of wood-waste tire rubber composite," *Compos. Sci. Technol.* 70(14), 2033-2038. DOI: 10.1016/j.compscitech.2010.03.015
Zhao, J., Wang, X.-M., Chang, J.-M., and Zheng, K. (2008). "Optimization of processing variables in wood-rubber composite board manufacturing technology," *Bioresource Technol.* 99(7), 2384-2391. DOI: 10.1016/j.biortech.2007.05.031
Zhao, J., Wang, X.-M., Chang, J.-M., Zheng, K., Yao, Y., and Cui, Q. (2011). "Interaction and correlation of variables on wood-rubber functional composites manufacture," *Scientia Silvae Sinicae* 47(3), 146-155.

Article submitted: September 23, 2017; Peer review completed: January 6, 2018; Revised version received and accepted: January 15, 2018; Published: March 14, 2018.
DOI: 10.15376/biores.13.2.3300-3314